Soft Matter

PAPER

View Article Online
View Journal | View Issue



Cite this: *Soft Matter*, 2025, **21**, 3527

# Training allostery-inspired mechanical response in disordered elastic networks

Savannah D. Gowen *

Received 12th November 2024,
Accepted 3rd April 2025

DOI: 10.1039/d4sm01340a

rsc.li/soft-matter-journal

Disordered elastic networks are a model material system in which it is possible to achieve tunable and trainable functions. This work investigates the modification of local mechanical properties in disordered networks inspired by allosteric interactions in proteins: applying strain locally to a set of source nodes triggers a strain response at a distant set of target nodes. This is demonstrated first by using directed aging to modify the existing mechanical coupling between pairs of distant source and target nodes, and later as a means for inducing coupling between formerly isolated source-target pairs. The experimental results are compared with those predicted by simulations.



## 1. Introduction

The creation of novel artificial materials can often benefit from mimicking the robust abilities of materials found in living matter.[1] Rapid developments in materials science are increasingly pushing such capabilities through the development of biomimetic materials,[2] including materials that can heal,[3] learn,[4,5] and store memory.[6] Included in this genre of materials are those that can be trained to perform unique functions that were not specifically designed into them at the outset:[7] One base material can be trained for a variety of different tasks. This allows for significant flexibility in the material function. Extensive research is needed to determine the limits of adaptable function through training in non-living matter.

One biological example of unusual function comes from a phenomenon in protein dynamics called allostery: the binding of a molecule at one site in a protein triggers the ability of a distant site to bind to another molecule.[8] This action-at-a-distance is one important way that proteins control their activity. Recent work has demonstrated the possibility of creating non-biological materials that mimic allosteric behavior.[9–12]

Rocks *et al.* modeled elastic materials as disordered spring networks, which are composed of central-force spring bonds connected at nodes in a disordered array.[9] Through the process of pruning selected bonds, they showed that distant sites on the network can be mechanically coupled to move either in-phase or out-of-phase with one another. Once designed, they showed that these tuned networks could be fabricated in the laboratory with physical materials. A similar function can be achieved in networks of tunable beam elements where local network properties are modified by actively updating beam stiffness.[13] However, these approaches require knowledge of the network's global properties to tune such function; this becomes prohibitive in the design or fabrication of arbitrarily large networks.

Allosteric function can be achieved without extensive computation by implementing tuning based on local training rules.[12,14,15] For example, networks of coupled adaptive units can be designed to update their rest lengths by contrasting their current state with that of a desired output configuration.[12] Similarly, for a continuous material network, Pashine described a bond pruning procedure that relies on observation of local stress-induced birefringence in a quasi-two-dimensional photoelastic network.[15] However, designing individual adaptive units that obey well-defined learning rules requires some engineering prowess and procedures like bond pruning remain time-consuming in practice and are limited to materials that are optically responsive to force.

Another approach, inspired by bond pruning, but which does not require the actual removal of any bonds or any direct computation of the material's elastic properties, is referred to as directed aging.[16] This method is a form of training that takes advantage of a material's innate ability to adapt to an applied stress load in time. This adaptation could be through the progressive weakening of bonds or the initiation of instabilities such as buckling to lower the energy of the directed state. Once aging is complete, the material should ideally respond according to how it was strained in the training process.

The success of directed aging was demonstrated in the creation of materials with negative Poisson's ratios. Most naturally occurring materials have a positive Poisson's ratio, $\nu > 0$, so that an applied strain in the material along one axis creates a strain of the opposite sign along its perpendicular axes. It is rare to find materials with $\nu < 0$, referred to as auxetic materials.[17] It was demonstrated both in simulations

*Department of Physics and The James Franck and Enrico Fermi Institutes, University of Chicago, Chicago, IL 60637, USA.*
*E-mail: savannah.gowen@mat.ethz.ch*

and experiments that by aging a disordered elastic network under a compressive strain, one can selectively lower the network's bulk modulus with respect to its shear modulus.[16,18] Because the Poisson's ratio is a monotonic function of the ratio of the bulk to shear moduli, this can eventually lead to a material with a negative Poisson's ratio.

Although directed aging has been demonstrated as an effective means for modifying global material properties like the Poisson's ratio, it is not clear that directed aging can lead to localized function in physical materials in the laboratory. A bulk response requires aging contributions from bonds throughout the network, while in the case of mechanical allostery, the source and target responses are confined to local regions of the material. Although simulations have suggested that directed aging can be implemented to modify a network's local mechanical properties,[18] until now this has not been attempted in real materials.

In this work, I use directed aging as a means of modifying the local mechanical coupling between separated sites in two-dimensional disordered networks. In the first example, I show that this type of training can be used to reduce the mechanical coupling between separated pairs of nodes that were initially coupled. In a second example, I use training to induce a desired coupling between node pairs that were originally mechanically uncoupled. I compare these experimental outcomes to those previously observed in simulations.

## 2. Experimental protocol

Disordered elastic networks are fabricated by laser cutting network designs derived from simulated two-dimensional jammed particle packings into a solid sheet of EVA (ethylene-vinyl acetate) foam. A set of two source and two target nodes are arbitrarily selected and labeled as shown in Fig. 1. Initially, strain is applied to the source nodes as defined by $\varepsilon_s \equiv \Delta s/s$, where $s$ is the initial distance between the two source nodes and $\Delta s \equiv s_f - s$, the difference between final and initial node distances. The strain on the target nodes is measured in response as $\varepsilon_t \equiv \Delta t/t$ where $t$ is the initial distance between the two target nodes and $\Delta t \equiv t_f - t$, is the difference between the final and initial target node distances. The relative degree of coupling between distant node sites can be determined by measuring the ratio of the target to source strain:

$$\eta \equiv \varepsilon_t/\varepsilon_s \quad (1)$$

Here $\eta \approx 0$ indicates uncoupled nodes, while $|\eta| > 0$ indicates coupled node pairs with a mechanical response that is either in-phase ($\eta > 0$) or out-of-phase ($\eta < 0$).

Networks are trained *via* directed aging by applying a strain to the source and target node pairs for a fixed amount of time either statically or through (in-phase) cyclic driving (see Methods section for details). Cyclic driving is a means of training the source and target over a continuous range of strain values. After a fixed aging time, $\tau_{age}$, has elapsed, the constrained nodes are released, and the target strain is measured as a function of the varied source strain.

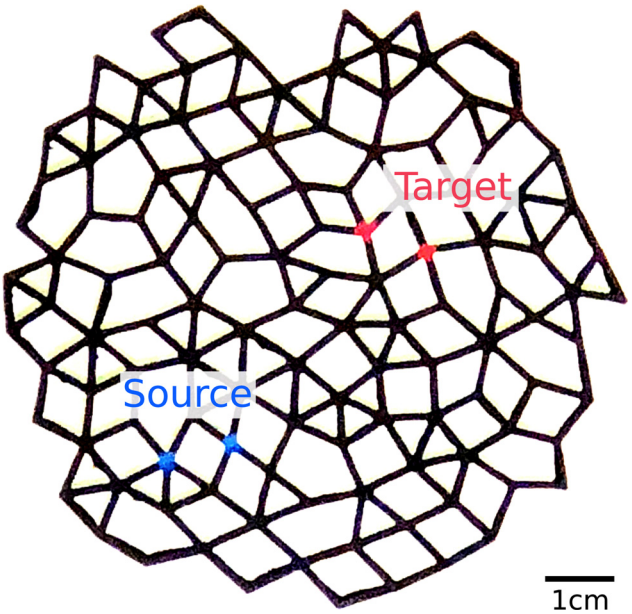


Fig. 1 Disordered elastic foam network labeled with source and target node pairs.

## 3. Results

Experimentally modifying the local mechanics of these networks is challenging because there is no simple means of quantifying how stress is distributed in the material when strain is locally applied. Changes in geometry through node displacements, bond bending, and buckling are indicative of concentrated stress but are difficult to quantify.

The first experiments reported here take pairs of nodes that are already mechanically coupled and use directed aging to decouple their interactions. Networks are derived from jammed particle packings and there is a chance that some pairs of source and target nodes are coupled once created. I take advantage of this feature by selecting node pairs with existing interactions for training from five distinct network geometries. The second set of experiments uses aging techniques to establish mechanical coupling in pairs of nodes that were initially non-interacting.

### 3.1. Suppressing node coupling *via* directed aging

Starting with source and target pairs that are mechanically coupled before any attempt to change the properties of the network (Fig. 2a), I apply a training protocol to decouple their motions. Once the coupled source and target nodes are determined, initial measurements of the strain ratio, $\eta_0$, are made by applying strains of approximately 0.25, 0.50, and 0.75 $\pm$ 0.10 to the source nodes and measuring the target strain response. One such measurement is shown in Fig. 2b.

To suppress the source-target interactions, I apply a large strain at the source while preventing the target nodes from reacting. This is accomplished by placing a physical barrier at the target to arrest strain at those nodes, as seen in Fig. 2c. The strain at the source can be applied either statically (that is, by

 

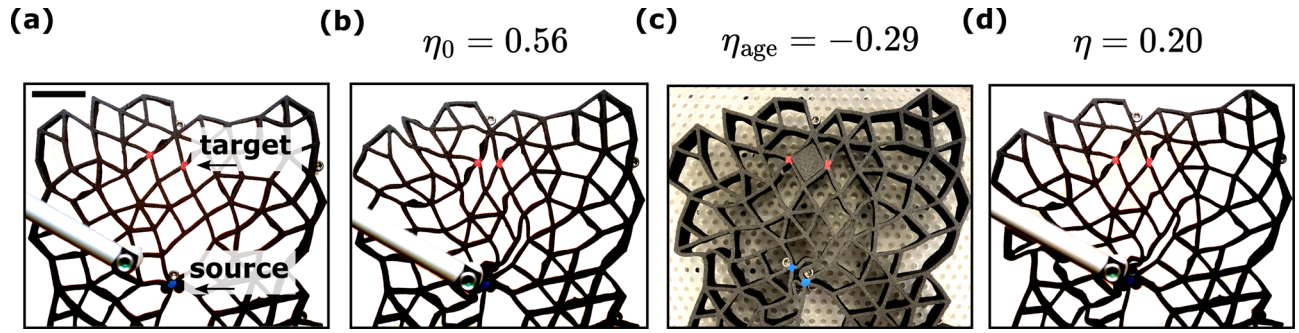


Fig. 2 Training protocol for suppressed node coupling *via* directed aging. (a) The source in the initially unstrained network is identified by one node painted blue and another below the screw seen at the end of the actuator shaft. The target nodes are denoted by two red dots. The scale bar represents 2 cm. (b) The initial strain-ratio, $\eta_0$, of the coupled source-target pair is measured. The source is strained by approximately 0.75. The target contracts in response. (c) To age the network, the source nodes are held compressed while the target is prevented from contracting (and is mildly stretched) by the insertion of a foam barrier resulting in a negative aging strain ratio, $\eta_{age}$. The network remains statically in this configuration for a fixed time, $\tau_{age}$. (d) The aged network is measured here at $\tau_{age}$ = 24 h. Aging has led to visibly less contraction of the target when the same strain is applied to the source.

constraining the source nodes to a constant applied strain) or cyclically (by oscillating the strain at the source to a fixed maximum amplitude to continuously vary the aging strain). These constraints are applied for a fixed aging time, $\tau_{age}$, then released, and the response $\eta$ is measured. An example of this is shown in Fig. 2d.

Fig. 3 shows the evolution of coupled source and target strains as a function of $\tau_{age}$, for a single network. Source and target strains appear linearly coupled. The strain ratio, $\eta$, given by the slope of the line, decreases as a function of $\tau_{age}$ until saturation at or before 24 hours. The inset shows $|\eta|$, the strain ratio, as a function of $\tau_{age}$ at the largest source strain. These experiments were repeated for five distinct network geometries which featured different connectivity and void fraction, and for multiple coupled source-target pairs. After aging, 75% of the networks showed a reduction in strain ratio by a factor of at least 0.5, and all networks decreased by a factor of at least 0.25. Less successful source-target pairs often had source and/or target nodes located on the boundary.

The specific aging protocol has a relatively small effect on the training outcome: Source-target pairs show decreased coupling for a range of input strains independent of whether aging was applied *via* a fixed strain or continuously through cyclic driving. Fig. 4 compares the same network aged either statically

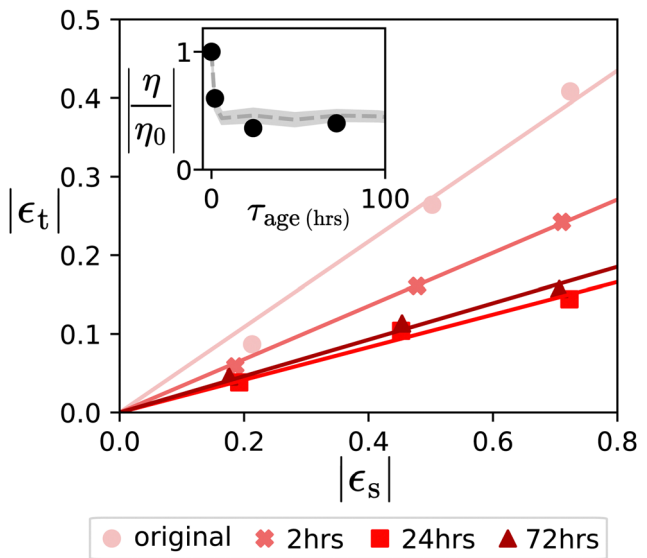


Fig. 3 Suppression of source-target strain coupling. The target strain, $\varepsilon_t$, is measured as a function of the source strain, $\varepsilon_s$, for varied aging times, $\tau_{age}$, (represented by different colors and markers) for the network imaged in Fig. 2. The strain ratio scaled by its initial value $\left|\frac{\eta}{\eta_0}\right|$ is computed for the largest source strains and is shown in the inset as a function of $\tau_{age}$. The strain ratio decreases as a function of time with a signal suppression that saturates at or before 24 hours of static aging. The gray region represents the average and standard deviation over samples with varied geometries and/or source-target pairs.

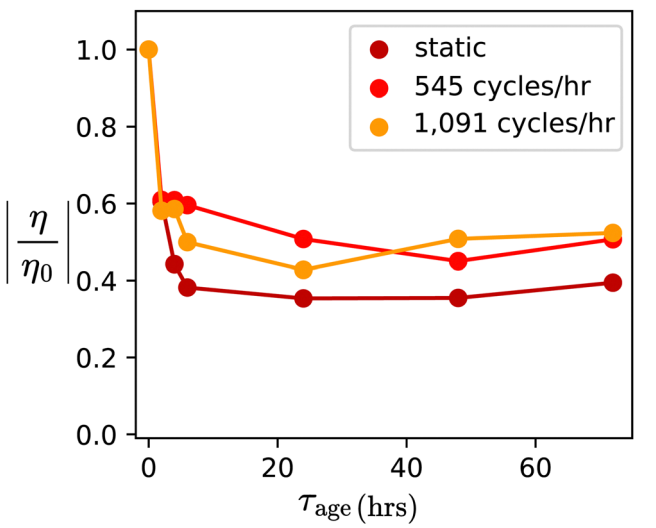


Fig. 4 Static *versus* cyclic training. The aged strain ratio, $\eta$, measured at the largest source strain is scaled by the initial strain ratio, $\eta_0$, for source and target nodes aged using three different protocols. One copy is aged statically while the other two alternate between static and cyclic activation as described in the text. All networks are aged for the same net aging time, $\tau_{age}$. The number of training cycles appears to have a negligible effect on the training outcomes, however, networks held static for a longer duration show marginally better results.

or *via* cyclic driving. The aged strain ratio, $\eta$, scaled by the initial strain ratio, $\eta_0$, is plotted as a function of aging time, $\tau_{age}$, for a network aged statically for the entire duration, one aged cyclically for 1/3 of that time and then held statically for the remainder, and another aged cyclically for 2/3 of that time and statically for the rest.

Despite the number of cycles differing by a factor of two or more, there is very little difference in the aging behavior of the three networks. Rather, networks aged statically for a longer fraction of the time appear to yield slightly better results.

Suppressing local mechanical coupling through aging is demonstrated here for both in-phase and out-of-phase interactions between the source and target. Although most experiments include a target that is prevented from compressing when source strain is applied, it is also possible to prevent target nodes from expanding by applying constraints. Directed aging thus appears to provide a robust method for modifying local stress distributions in the material.

### 3.2. Induced node coupling *via* directed aging

Inducing coupling between distant nodes introduces a more formidable challenge than modifying existing ones. When strain is applied locally to a source chosen at random, surrounding nodes will be displaced leading to bond bending and buckling in the region surrounding the source. Previous work shows that there is a length scale, $\xi$, associated with the decay of local stress that depends on the network coordination.[19] For directed aging to work effectively, stress applied to the source and target must affect a set of common bonds,[15,18] and this is not possible if the distance between the source and target is too large, and/or if $\xi$ is too small. Because $\xi$ cannot easily be measured in the experiment, targets are chosen by straining the source and locating target nodes that are close by, but which remain unaffected when the source is strained. This procedure is used to select source and target nodes from six distinct geometries. Fig. 5a shows one such example. Strain applied at the source has little effect on the target initially (Fig. 5b). The network is trained by applying a large negative (compressive) strain to both the source and target and allowing the network to age either statically (Fig. 5c) or by cyclic driving. The rest of the network remains unperturbed for the duration of the training. The network is then remeasured after aging (Fig. 5d).

Fig. 6a shows the evolution of source and target strain as a function of training time, $\tau_{age}$, for one example. Initially, the target strain, $\varepsilon_t$, remains constant as the source is strained such that the original data can be functionally described by $\varepsilon_t = 0$, as one would expect for uncoupled nodes. As the aging time, $\tau_{age}$, increases, we see that the source and target become increasingly coupled with $\varepsilon_t$ growing as a function of $\varepsilon_s$. This is further demonstrated by observing the strain ratio, $\eta$ as a function of $\tau_{age}$ at the largest source strains in Fig. 6b. Fig. 6c shows the maximum output strain ratio, $|\eta_{max}|$ for four copies of the same network aged at different imposed target strains. All four networks demonstrate successful coupling, however, the network with the largest output strain ratio was aged under the largest strain. This further motivates training at maximal strain values.

This protocol is repeated for six different network geometries and a variety of source-target pairs. The strain ratio for each uncoupled network is initially $0 \pm 0.05$. Successful coupling is defined when the strain ratio increases to $|\eta| \geq 0.1$ for any of the applied source strains. Successful coupling was achieved for 73% of experiments. The average and standard deviation for these networks is shown by the dotted gray and surrounding gray lines in Fig. 6b respectively. It should be noted that unlike in the previous set of experiments, here strain interactions in the network can behave non-linearly such that it is possible to measure coupling at one value of the source strain but not necessarily at another. I generally observe that the largest coupling is present at the greatest applied source strain value, but not exclusively so.

Some source-target pairs fail to couple the input and output response. Reasons for failure may include attempting to couple nodes that are sufficiently far from each other as compared to the decay length of local stresses, $\xi$. Failure is also more likely when the target is located too close to a constrained source node. In this case, some nearby bonds may be prevented from transmitting stress and thus impede node coupling. This may also come from the fact that stress around a point source in

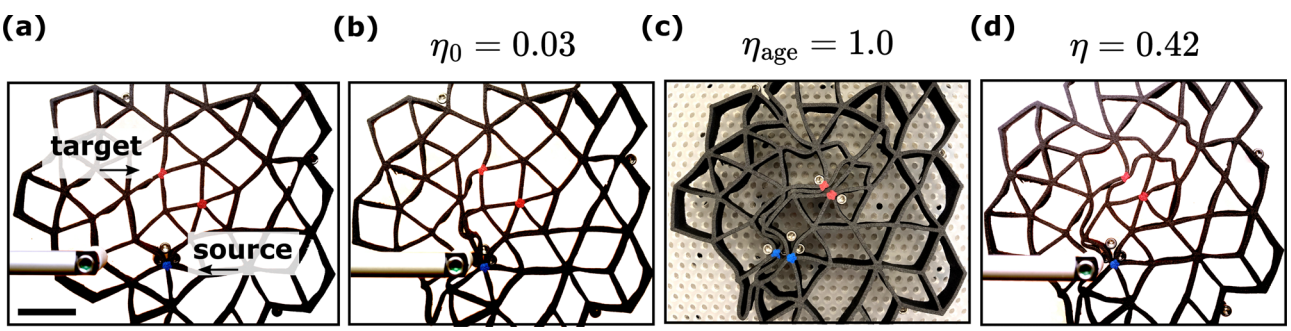


Fig. 5 Training protocol for inducing node coupling *via* directed aging. (a) An uncoupled source and target pair are chosen. The scale bar represents 2 cm. (b) The initial strain-ratio measurement is taken. When the source is strained by approximately 0.75, the distance between target nodes (red dots) is relatively unchanged. The initial strain ratio, $\eta_0$, is approximately 0. (c) Directed aging is shown by applying compression statically to the source and target nodes for a set duration, $\tau_{age}$. (d) The aged network is measured at $\tau_{age}$ = 7 days. The aged target now contracts in response to an applied source strain, yielding a positive strain ratio.

 

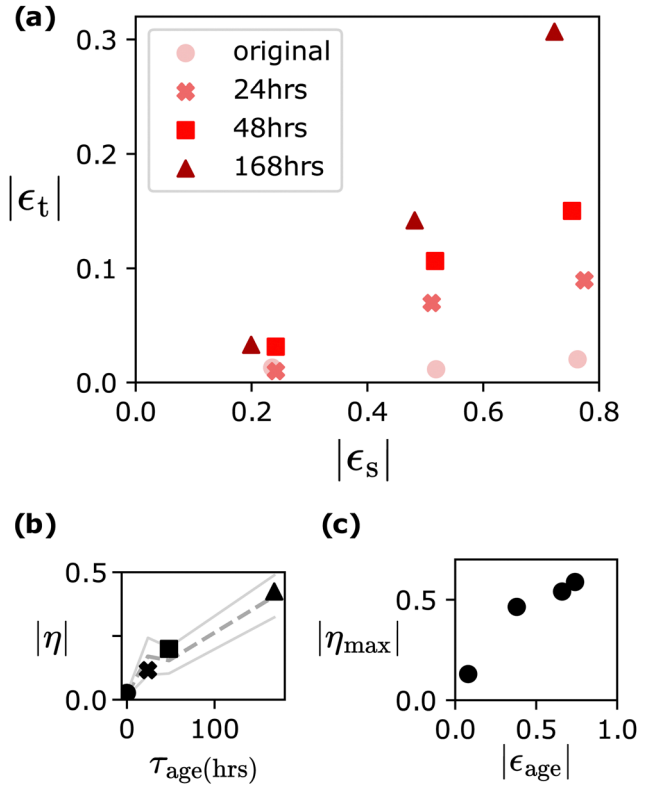


Fig. 6 Induced node coupling as a function of aging time, $\tau_{age}$. (a) The target strain, $\varepsilon_t$, increases as a function of source strain, $\varepsilon_s$, with progressive aging time (indicated by different colors and markers) for the network imaged in Fig. 5. (b) The strain ratio, $|\eta|$, is measured at the largest source strain values and increases from a value of 0 (uncoupled nodes) to roughly 0.5 (coupled nodes) with $\tau_{age}$ The average and standard deviation over other network geometries in shown in gray. (c) The maximum strain ratio, $|\eta_{max}|$, is measured as a function of the target aging strain, $\varepsilon_{age}$, for four copies of the network shown in Fig. 5 aged at different strains. The largest induced strain ratio corresponds with the largest aging strain.

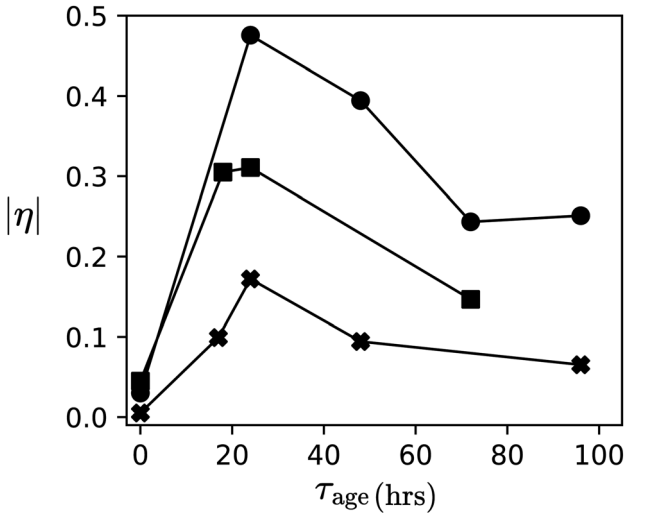


Fig. 7 Over-trained networks. The strain ratio, $|\eta|$, is shown as a function of aging time, $\tau_{age}$, at high source strains for three different experiments (indicated by different markers). The curves shown with square and circular points are two copies of the same source-target pair, while the crosses represent another source-target pair. $\eta$ reaches a maximum value, or maximum coupling, at some intermediate time and then falls non-monotonically.

these systems can be highly anisotropic.[19] Among other failure modes were those in which the target nodes were trained under large tensions to induce node expansion. These bonds appear to have undergone such significant plastic deformation that they became highly uncoupled from the rest of the network. Inducing target node expansion might still be accomplished with lower aging strains but further exploration is necessary.

Networks trained both statically or cyclically could successfully couple source and target nodes. However, static aging consistently yielded a stronger coupling for the same aging time.

### 3.3. Over-training

The training for allosteric response is not always monotonic in time. For over a quarter of experiments, if aged for too long, the coupling response can deteriorate. Thus, in some networks, $|\eta|$ was maximum at an intermediate time, as shown by a few examples in Fig. 7. This response seems more common for networks containing bonds with high aspect ratios. During aging, material struts under large stress loads buckle; sustaining this buckling for long periods can result in material fatigue which then drastically weakens the elastic response of the bond, rendering the training less effective. This effect is not unique to our system.[20] This decrease or plateau in the strain ratio is observed more frequently in networks aged for long durations, and should be observed in all networks if aged for long enough. This phenomenon is evidence that one can over-train a material, at which point, aging adopts the negative connotations that one may have naturally associated with the term.

## 4. Discussion

These experiments both validate the computational findings of Hexner *et al.*[18] and introduce a few notable differences. The simulations model elastic materials as disordered, central-force spring networks. The networks are aged by performing an energy minimization algorithm in which the rest length of each bond evolves with the stress applied to that bond when subjected to an applied strain. In their study, strain is applied cyclically while the networks age as a means of training the output signal for a range of input strains, rather than a single one. In these experiments, for both coupling and decoupling nodes, I find that static training is equally or more effective than cyclic driving. The majority of networks aged statically at a single large value of $\eta_{age}$ display the trained response at smaller strains as well. These results may imply that cyclic driving could be unnecessary to locally train networks over a range of source strain values.

The coupled interactions achieved in these experiments were significantly smaller in magnitude than those from simulations. In simulations, a large percentage of source-target pairs

could be trained to strain ratios of $\eta \approx 1$.[18] In experiment, the highest observed output strain ratio was $|\eta| = 0.64$. However, our results cannot be directly compared because the aging strains used in these experiments were larger than those considered in simulations, with a typical aging strain around $\varepsilon_s \approx 0.75$ *versus* 0.5 in simulations.

Additionally, Hexner *et al.* suggests that the inclusion of "repeaters", randomly chosen nodes throughout the network that are strained in addition to the source and target, could ameliorate the failure rate in training long-range targets.[18] In some cases, duplicating failed experiments with the inclusion of repeaters does lead to an induced coupling, but not consistently so. The dependence of coupling on the source to target distance, and the efficacy of repeaters in increasing the range of source-target interactions remain to be further investigated in these experimental systems.

Disparities between experimental and simulation results are likely due to the more complex adaptive behaviors of physical networks that are not accounted for in the computational models. Pashine *et al.* used directed aging to tune the Poisson's ratio for the same type of disordered EVA foam networks[16] and showed that the ability to train relies both on changes to bond stiffness and more significantly changes to the network geometry. For example, bond bending, the change in the angle at which bonds meet at a node, and bond buckling are also observed to be a critical adaptive mechanism in these experiments. Another feature of real materials that is not present in idealized spring models is the inclusion of pre-stress in bonds. Although the initial network is in static equilibrium, stresses may still exist in force balance with one another. It has been shown that the inclusion of even a small amount of pre-stress in spring models can have significant implications on the training outcomes.[21,22]

Previous characterization of the EVA foam used here suggests that training occurs *via* both plastic and viscoelastic adaptations of the material; these properties depend on the aging time and could be further tuned with the incorporation of temperature.[16] In these experiments, measurements are taken directly after aging, and thus on a time scale much shorter than the viscoelastic relaxation time of the material which is on the order of days or weeks.[16] Although EVA foam undergoes plastic deformation, in general, plasticity is not required for training as long as the desired output can be achieved on time scales that are much shorter than the relaxation time, much like in biological systems.

This work demonstrates experimentally that local material properties can be trained *via* directed aging. Mechanical coupling was reduced by at least 1/4 of the initial strain ratio for source-target pairs in 100% of the decoupling experiments. In the second set of experiments, although source-target nodes could not always be coupled to $|\eta| \geq 0.1$, the success rate was comparable to values previously reported. In experiments in which the same type of allosteric mechanical interactions were induced with bond pruning, Pashine reports success rates between approximately 70–90% for the same strain ratio values.[15] The inability to couple nodes through pruning was attributed to bond-bending and non-linearity in the stress–strain response of the material. These non-linear effects are likely significant to these experimental results as well. However, in simulations of directed aging there is a 10% failure rate even without these added complexities included in the computational model.[18] In this work, approximately 75% of source-target pairs are coupled by at least 10% after aging. The ability to train a relatively large fraction of source-target node pairs without the added insight of computation in experiment evidences the robust ability of disordered materials to adapt, and the promise of directed aging as a material design technique.

## 5. Methods

In these experiments, we use disordered network structures derived from 2D computer-simulated jammed particle packings. Each node corresponds to the center of a circular particle while bonds indicate particle contacts where circles overlap. This structure is then laser cut using a Universal Laser Systems Ultra X6000 into a solid sheet of ethylene-vinyl acetate (EVA) closed cell foam, with a density of 2 lbs per $ft^3$ and 0.5 in thickness from McMaster-Carr. Source and target node pairs are labeled with red and blue paint to facilitate strain measurements. To apply source and target strain, one source node is fixed while the strain is applied to the other using a linear actuator with feedback (Actuonix Motion Devices Inc.). Strain is applied at a roughly constant speed while the actuator is driven with a square wave signal. Network boundaries are constrained on a perforated platform with screws to inhibit global translation or rotation of the material while a strain is being applied. These constraints would presumably be unnecessary for an infinite system but are essential for reducing finite size effects while applying strain locally.

Source and target responses are captured for various source strains using a Nikon D7000 DSLR camera. Training *via* directed aging is applied cyclically by synchronizing actuators to apply strain at both the source and target nodes repeatedly, or statically by constraining the source and target nodes as desired for a fixed amount of time. Cyclic actuation is driven at a frequency of 450 mHz using a motor driver powered by an Arduino. For all measurements, the source nodes are forced back to their approximate initial positions.

## 6. Conclusions

The experiments reported here demonstrate that local mechanical coupling between distant pairs of nodes can be modified or induced *via* directed aging in disordered elastic network materials. The ability to tune a material's mechanical properties locally without large-scale computations or design presents a promising new direction for materials development that takes inspiration from modes of response in biological systems.

In disordered foam networks, by forcing the material into geometric configurations in which the source and target are actively strained and allowing them to age, the system evolves to a state in which these configurations become energetically favorable through the weakening of bonds under stress and *via*

 

changes in the effective bond lengths. This presumed material adaptation is dependent on the nature of the constituent material. For example, materials that are strain hardening may induce other novel training outcomes.

More work remains to characterize the material-based limitations of aging in network structures; For example, training under tension is less effective in foams due to a significant loss of elasticity. Preliminary experiments in which similar training was applied to 3D-printed elastomer networks led to fracture before training outcomes were achieved. Such cases of failed training might inspire further exploration for more effective aging protocols. For example, varying ambient temperature conditions could allow a more rapid aging response and longer memory of the training.

## Data availability

Data for this article, including raw source-target node distance measurements are available at Training-Mechanical-Allostery at **https://github.com/gowen22s/Training-Mechanical-Allostery/tree/main**.

## Conflicts of interest

There are no conflicts to declare.

## Acknowledgements

I would like to thank Nidhi Pashine for helpful advice and insightful discussions throughout the development of these experiments. I would also like to thank Samar Alqatari and Varda Hagh for their perspectives and guidance on the simulations. Finally, I would like to especially acknowledge the contributions of Sidney R. Nagel as an advisor and mentor throughout the development of this work. This research was supported by the University of Chicago Materials Research Science and Engineering Center, NSF-MRSEC program under award NSF-DMR 2011854.

## Notes and references

1 M. A. Meyers, P.-Y. Chen, A. Y.-M. Lin and Y. Seki, *Prog. Mater. Sci.*, 2008, **53**, 1–206.
2 B. Bhushan, Philosophical Transactions of the Royal Society A: Mathematical, *Phys. Eng. Sci.*, 2009, **367**, 1445–1486.
3 R. P. Wool, *Soft Matter*, 2008, **4**, 400–418.
4 M. Stern and A. Murugan, *Annu. Rev. Condens. Matter Phys.*, 2023, **14**, 417–441.
5 S. Dillavou, B. D. Beyer, M. Stern, A. J. Liu, M. Z. Miskin and D. J. Durian, *arXiv*, 2023, preprint, arXiv:2311.00537, DOI: **10.48550/arXiv.2311.00537**.
6 N. C. Keim, J. D. Paulsen, Z. Zeravcic, S. Sastry and S. R. Nagel, *Rev. Mod. Phys.*, 2019, **91**, 035002.
7 H. M. Jaeger, A. Murugan and S. R. Nagel, *Soft Matter*, 2024, **20**, 6695–6701.
8 H. N. Motlagh, J. O. Wrabl, J. Li and V. J. Hilser, *Nature*, 2014, **508**, 331–339.
9 J. W. Rocks, N. Pashine, I. Bischofberger, C. P. Goodrich, A. J. Liu and S. R. Nagel, *Proc. Natl. Acad. Sci. U. S. A.*, 2017, **114**, 2520–2525.
10 L. Yan, R. Ravasio, C. Brito and M. Wyart, *Proc. Natl. Acad. Sci. U. S. A.*, 2017, **114**, 2526–2531.
11 M. R. Mitchell, T. Tlusty and S. Leibler, *Proc. Int. Acad. Ecol. Environ. Sci.*, 2016, **113**, E5847–E5855.
12 L. E. Altman, M. Stern, A. J. Liu and D. J. Durian, *Phys. Rev. Appl.*, 2024, **22**, 024053.
13 R. H. Lee, E. A. Mulder and J. B. Hopkins, *Sci. Rob.*, 2022, **7**, eabq7278.
14 V. P. Patil, I. Ho and M. Prakash, *arXiv*, 2023, preprint, arXiv:2304.08711, DOI: **10.48550/arXiv.2304.08711**.
15 N. Pashine, *Phys. Rev. Mater.*, 2021, **5**, 065607.
16 N. Pashine, D. Hexner, A. J. Liu and S. R. Nagel, *Sci. adv.*, 2019, **5**, eaax4215.
17 W. Yang, Z.-M. Li, W. Shi, B.-H. Xie and M.-B. Yang, *J. Mater. Sci.*, 2004, **39**, 3269–3279.
18 D. Hexner, A. J. Liu and S. R. Nagel, *Proc. Int. Acad. Ecol. Environ. Sci.*, 2020, **117**, 31690–31695.
19 W. G. Ellenbroek, E. Somfai, M. van Hecke and W. Van Saarloos, *Phys. Rev. Lett.*, 2006, **97**, 258001.
20 C. Arinze, M. Stern, S. R. Nagel and A. Murugan, *Phys. Rev. E*, 2023, **107**, 025001.
21 A. Matthews, S. Nagel and M. Gardel, Training Networks with Internal Prestress, *APS March Meeting Abstracts*, 2023, T10.009.
22 X. Li, J. Liu and A. K. Soh, *Int. J. Fract.*, 2024, **246** 225–244.